

# Cretaceous–Tertiary Rhenodanubian flysch wedge (Eastern Alps): clues to sediment supply and basin configuration from zircon fission-track data

Britta Trautwein,\* István Dunkl, Joachim Kuhlemann and Wolfgang Frisch

*Institut für Geologie und Paläontologie, Sigwartstr. 10, 72076 Tübingen, Germany*

## ABSTRACT

The provenance of Cenomanian to Eocene flysch deposits accreted along the northern margin of the Eastern Alps has been investigated by means of zircon fission-track (FT) geochronology and zircon morphology. The Rhenodanubian flysch and Ybbsitz klippen zone comprise several nappes representing the Main flysch and Laab basins. The Laab basin received sediments of stable European provenance, indicated by pre-Variscan, Variscan, and Permian–Triassic zircon FT ages, and was thus located in the immediate south of the European margin. The Main flysch basin was supplied

mainly from the evolving Eastern Alps and was therefore situated south of the Laab basin. Zircon populations with Permian to Jurassic cooling ages in the Main flysch basin are related to increased heat fluxes during the break-up of Pangaea and are probably derived from the northwestern part of the Eastern Alps. The dominant Cretaceous zircon FT cooling ages reflect Eoalpine metamorphism in the Austroalpine realm.

*Terra Nova*, 13, 382–393, 2001

## Introduction

On the basis of heavy mineral and sedimentological data, several palaeogeographical reconstructions for Cretaceous–Tertiary times have been proposed for the Rhenodanubian flysch zone (RDFZ) of the Eastern Alps (e.g. Hesse, 1973; Frisch, 1979; Egger, 1995; Oberhauser, 1995). Modern provenance studies use zircon fission-track (FT) geochronology as a powerful tool to define the thermotectonic evolution and exhumation of the source area of the sediments (Brandon, 1992). Zircon FT ages reflect the thermal processes of the upper 8 km during exhumation, owing to a closure temperature of  $240 \pm 50$  °C (Hurlford, 1986). The comparison of zircon ages of ancient sedimentary units with those of actually exposed rocks in possible source areas provides information about the provenance and elucidates the palaeogeography.

The aim of the present study is to demonstrate that zircon FT studies provide excellent clues for unravelling the provenance and palaeogeography of flysch basins in a case study of the Eastalpine RDFZ.

## Geological setting

The RDFZ forms a narrow zone along the northern front of the Eastern Alps and is overthrust onto the Molasse basin and the Bohemian massif (BM) belonging to stable Europe (Fig. 1). Parts of the Austroalpine nappe stack of the Eastern Alps and the BM consist of amphibolite-facies metamorphic rocks and late Palaeozoic granitoids. Both areas were affected by the Variscan orogeny, post-Carboniferous unroofing (Hejl *et al.*, 1997) and Permian–Jurassic thermotectonic processes resulting from the disintegration of Pangaea (Ziegler, 1988). Only the Austroalpine units of the Eastern Alps were involved in the Eoalpine orogeny which was followed by cooling in Cretaceous times (Fig. 2a,b; Frank *et al.*, 1987; Hoinkes *et al.*, 1999; Thöni, 1999). Finally, the Alps were involved in Tertiary collision of the Adriatic plate with the European foreland by closure of the Penninic ocean. During subduction and collision, the Rhenodanubian flysch (RDF) became accreted.

According to the palaeogeographic position of the RDFZ between the Austroalpine zone and the BM, these two realms have been proposed as source areas for the flysch deposits (e.g. Oberhauser, 1995).

The Penninic RDFZ represents an Early Cretaceous to early/middle Eocene turbiditic sequence (Egger, 1992; Schnabel, 1992) (Fig. 2c). The

Ybbsitz klippen zone (YKZ) was part of the Penninic oceanic basement (Schnabel, 1992) and consists of Jurassic ophiolites and a Cretaceous sequence similar to the RDF (Ruttner and Schnabel, 1988; Decker, 1990; Schnabel, 1992).

The RDFZ is strongly sliced and tectonically disrupted. The Main Flysch nappe stretches over 500 km from the Rhine to the Danube river. For instance, at the eastern termination (Wienerwald) the RDFZ is subdivided into three nappes (Fig. 2a): the Greifenstein nappe, which is the equivalent of the Main Flysch nappe (Schnabel, 1992), is overlain by the Laab nappe in the south and the Kahlenberg nappe in the south-east (Prey, 1983).

## Methods

FT geochronology was performed on 21 zircon samples of Cenomanian to Eocene age of the RDFZ and the YKZ (Table 1). FT dating on detrital zircons yields age spectra that give information about the thermotectonic evolution in the source area. The age spectra were decomposed into finite sets of age populations using the program Binomfit (Brandon, 1992), which is based on the binomial peak-fitting method of Galbraith and Green (1990).

## Results

Modelling of zircon FT age spectra reveals several zircon FT age popula-

\*Correspondence: Britta Trautwein, Institut für Geologie und Paläontologie, Sigwartstr. 10, 72076 Tübingen, Germany. Tel.: +49 7071 2974702; fax: +49 7071 5059; email: britta.trautwein@uni-tuebingen.de

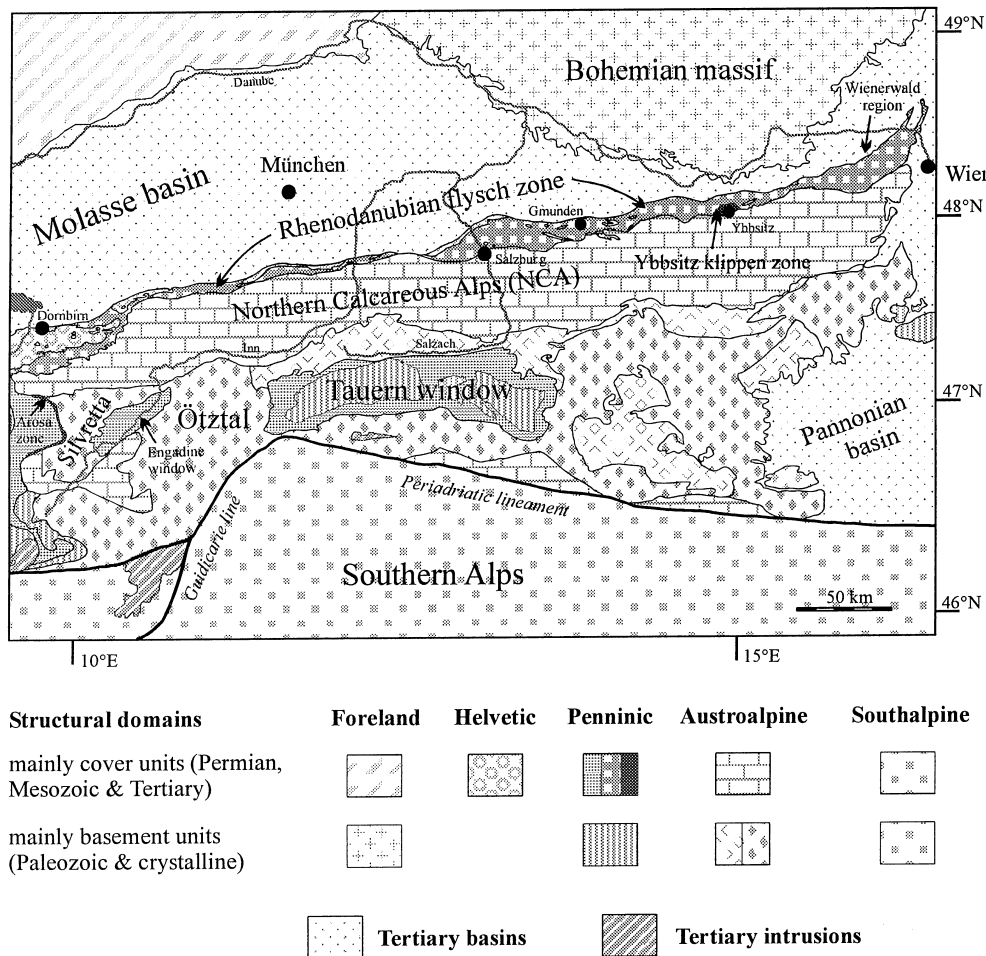


Fig. 1 Geological map of the Eastern Alps.

tions (Fig. 3, Table 1), which provide information about the catchment area. Post-sedimentary thermal overprint of the zircons can be excluded, because vitrinite reflectance data reach max. 0.9% Rr in the Wienerwald (Gmach, 1999) and 0.7% Rr in the western RDFZ (Petschick, 1989). The age cluster show some systematic change with stratigraphic age of the sediments but are otherwise uniform in all units except the Laab nappe. The youngest cluster becomes generally more recent with decreasing stratigraphic age, indicating exhumation of the source area. However, the trend is absent in the Laab nappe, which demands a different explanation.

*Cenomanian–Turonian (97–89 Ma)*

Uniform zircon FT age populations of Early Cretaceous and Permian–

Triassic age are characteristic for the Cenomanian–Turonian formations (Fig. 4a), with two exceptions showing a Jurassic and no Cretaceous age cluster (sample AL14, YB3). The Early Cretaceous ages are a characteristic of the Austroalpine realm and reflect the cooling after Cretaceous Eoalpine metamorphism (Fig. 2a, b). Thus, a southern catchment area is assumed for the Reischelsberg Formation, which is in line with palaeocurrent data (Mattern, 1998). Samples AL4 and YB3 are possibly derived from those parts of the Austroalpine basement that experienced no or very weak Alpine overprint, such as the northwestern Silvretta and Ötztal basement (Fig. 2a, b; Neubauer *et al.*, 1999; Thöni, 1999). The Jurassic zircon FT age population is interpreted to reflect heating during rifting and opening of the Penninic ocean, which

affected Austroalpine and South-Alpine units (von Eynatten, 1996; Bertotti *et al.*, 1999; Dunkl *et al.*, 1999; Schuster *et al.*, 1999; Vance, 1999). The Permian–Triassic ages are related to the Permian–Triassic extensional phase in Europe (Ziegler, 1988) with enhanced heat flow resetting the zircon FT system (Bertotti *et al.*, 1999; Schuster *et al.*, 1999). Therefore, these ages are not discriminative, but may indicate both an Alpine and a European source.

*Santonian–Campanian (87–74 Ma)*

In contrast to continuous trends in the other nappes (samples OA3, WW4, WW7; Fig. 4b, Table 1), the Kaumberg Formation (Laab nappe) yields only zircons of late Jurassic and Permian FT ages (WW13, Fig. 4b, Table 1). Thus, the basin received

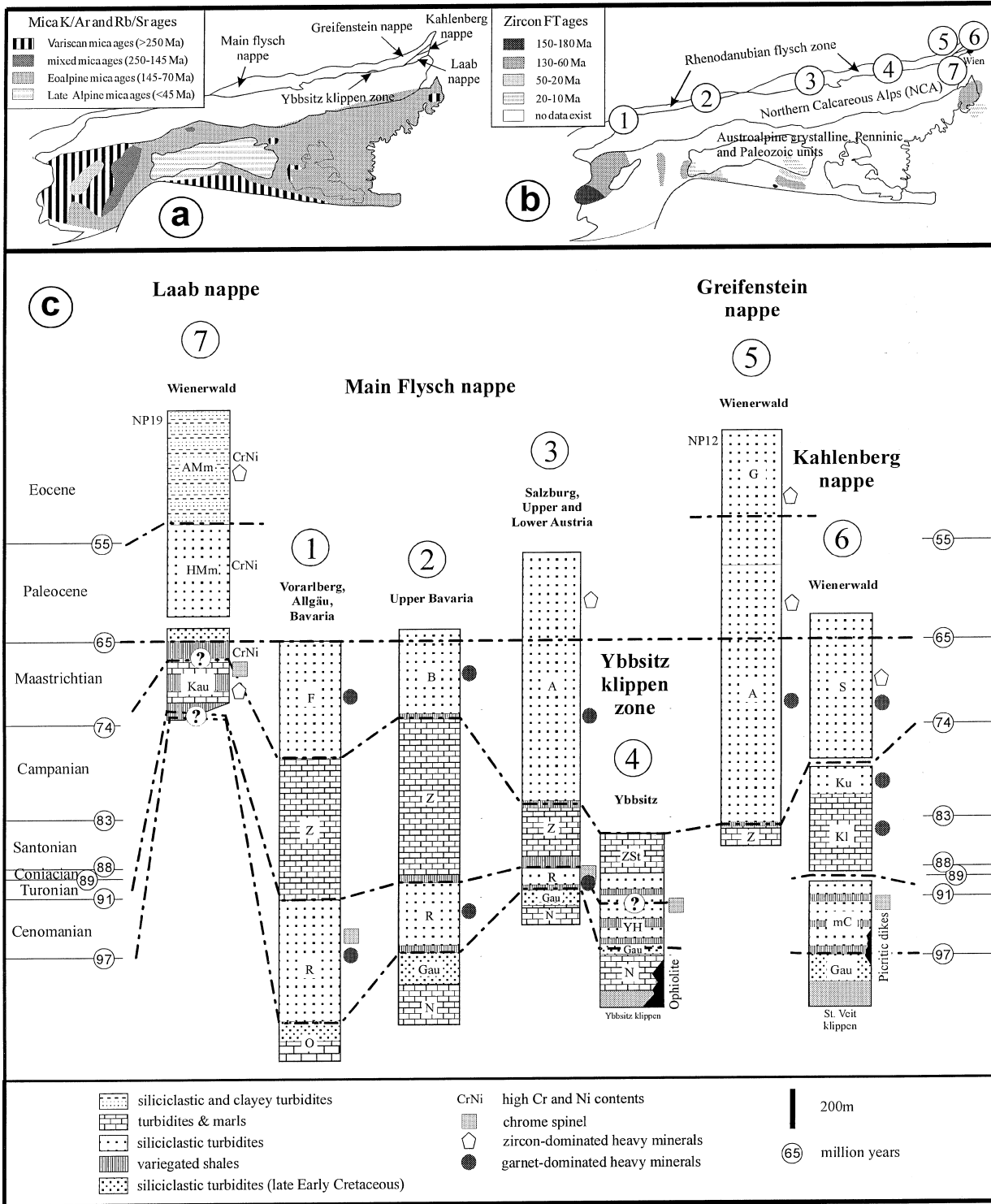


**Fig. 2** (a, b) Compilation of mineral cooling ages in the Eastern Alps (see Brügel, 1998). (c) Facies development in the nappes of the Rhenodanubian flysch zone and the Ybbsitz klippen zone (compilation after Prey, 1973; Schnabel, 1992; Oberhauser, 1995; Faupl, 1996). A, Altenglach formation; Amm, Agsbach Member; Gau, Gault Flysch; G, Greifenstein Formation; HMm, Hois Member; Kau, Kaumberg Formation; Kl, lower Kahlenberg Formation; Ku, upper Kahlenberg Formation; mC, mid-Cretaceous formations (undifferentiated); N, Neocom Flysch; O, Ofterschwang Formation; R, Reischelsberg Formation; S, Sievering Formation; YH, Ybbsitz Formation including Hubberg Formation; Z, Zementmergel Formation; ZSt, Zementmergel Formation including Steinkeller Formation; NP12, NP19, nannoplankton zones.

**Table 1** Zircon fission-track data and modelled age clusters using the computer program Binomfit (Brandon, 1992). The ages were calculated using dosimeter glass CN-2 and a  $\zeta$ -factor of  $122.5 \pm 1.4$ . The  $\zeta$ -value was calculated from 13 different age standards of Fish Canyon Tuff, Buluk Member, and Tardree Rhyolite zircons irradiated during seven different reactor runs (Trautwein, 2000) at the nuclear reactor RISO in Roskilde, Denmark. The external-detector method (Gleadow, 1981) was used with low uranium mica as detector. Per zircon sample two mounts were prepared. The two mounts of WW7 and HAMfo4 were in different irradiations resulting in different  $\rho_d$  therefore the two aliquots are mentioned separately (a and b). The majority of the zircon samples was etched using a KOH-NaOH eutectic liquid at 215 °C (Gleadow et al., 1976) for 23–31 h. A minority of the samples (WW1, ÖGAI1, MSRsl, ZKRsl, ZKRsl, some mounts of HAMfo4 and WW7) was etched in a molten LiOH\*H<sub>2</sub>O-KOH-NaOH eutectic mixture at 200–205 °C

Sample No.	Sediment age [Myr]	Locality N, E	No. of Crystals	Spontaneous tracks			Induced tracks			Dosimeter glass			Age populations			Fit statistics
				$\rho_s$ [10 <sup>5</sup> cm <sup>-2</sup> ]	$N_s$	$\rho_i$ [10 <sup>5</sup> cm <sup>-2</sup> ]	$M_i$	$\rho_d$ [10 <sup>5</sup> cm <sup>-2</sup> ]	$N_d$	Age $\pm 1\sigma$ [Myr]	$N_i$	$W$ [%]	1	2	3	
<b>Main flysch/Greifenstein nappe</b>																
AL4	Ma	47°50', 11°40'	60	199.0	5864	61.8	1820	6.56	1284	70 $\pm$ 6 $N_i$ = 12.5 $W$ = 22%	122 $\pm$ 9 $N_i$ = 30.4 $W$ = 24%	247 $\pm$ 20 $N_i$ = 17.1 $W$ = 30%	$\chi^2$ = 59 $\nu$ = 55	$P(F_{1,\nu})$ = 0% $F$ = 12.26		
AL14	Ce–Tu	47°32'42", 10°25'08"	60	315.4	7665	62.3	1515	6.62	1304	183 $\pm$ 10 $N_i$ = 44.5 $W$ = 24%	293 $\pm$ 38 $N_i$ = 15.5 $W$ = 29%	–	$\chi^2$ = 69 $\nu$ = 57	$P(F_{1,\nu})$ = 0% $F$ = 40.88		
HAMfo4 a	Ma	47°55'15", 13°45'55"	39	124.2	3541	23.4	667	5.14	1020	88 $\pm$ 9 $N_i$ = 8.2 $W$ = 25%	208 $\pm$ 13 $N_i$ = 30.8 $W$ = 34%	–	$\chi^2$ = 44 $\nu$ = 36	–		
b			21	199.4	2374	56.5	673	6.44	1284	72 $\pm$ 5 $N_i$ = 8.1 $W$ = 21%	216 $\pm$ 15 $N_i$ = 12.9 $W$ = 26%	–	$\chi^2$ = 21 $\nu$ = 18	–		
ÖGAI1	Ma	47°51'06", 13°17'53"	60	229.4	6462	36.6	1031	5.44	1075	95 $\pm$ 7 $N_i$ = 13.5 $W$ = 28%	254 $\pm$ 12 $N_i$ = 46.5 $W$ = 32%	–	$\chi^2$ = 63 $\nu$ = 57	–		
MSRsl	Ce–Tu	47°48'35", 13°25'05"	51	197.0	3712	36.2	683	5.45	1075	124 $\pm$ 12 $N_i$ = 17.8 $W$ = 31%	233 $\pm$ 18 $N_i$ = 33.2 $W$ = 38%	–	$\chi^2$ = 45 $\nu$ = 48	–		
ZKRsl	Ce–Tu	47°47'02", 12°40'28"	59	127.6	4131	27.8	899	5.14	1020	112 $\pm$ 9 $N_i$ = 32.9 $W$ = 30%	217 $\pm$ 28 $N_i$ = 26.1 $W$ = 39%	–	$\chi^2$ = 70 $\nu$ = 56	–		
OA1	Pa–Eo	48°04'16", 15°28'58"	60	303.6	8283	58.2	1588	6.67	1325	75 $\pm$ 8 $N_i$ = 4.2 $W$ = 20%	169 $\pm$ 22 $N_i$ = 21.1 $W$ = 27%	286 $\pm$ 25 $N_i$ = 34.6 $W$ = 27%	$\chi^2$ = 63 $\nu$ = 55	$P(F_{1,\nu})$ = 0% $F$ = 12.4		
OA3	Ca–Ma	47°59'49", 14°55'58"	41	262.4	5206	75.8	1503	6.47	1304	73 $\pm$ 6 $N_i$ = 8.3 $W$ = 19%	142 $\pm$ 8 $N_i$ = 23.1 $W$ = 22%	271 $\pm$ 24 $N_i$ = 9.6 $W$ = 29%	$\chi^2$ = 41 $\nu$ = 36	–		
YB2	Ce–Tu	47°58'51", 14°52'43"	15	416.7	2232	74.5	399	6.46	1304	101 $\pm$ 17 $N_i$ = 2.4 $W$ = 22%	252 $\pm$ 18 $N_i$ = 12.6 $W$ = 25%	–	$\chi^2$ = 19 $\nu$ = 12	–		

Table 1 Continued

Sample No.	Sediment age [Myr]	Locality N, E	No. of Crystals	Spontaneous tracks		Induced tracks		Dosimeter glass			Age populations			Fit statistics
				$\rho_s$ [ $10^5 \text{ cm}^{-2}$ ]	$N_s$	$\rho_i$ [ $10^5 \text{ cm}^{-2}$ ]	$N_i$	$\rho_d$ [ $10^5 \text{ cm}^{-2}$ ]	$N_d$	Age $\pm 1\sigma$ [Myr]	$N_f$	$W$ [%]	1	
WW1	Eo	48°20'57", 15°15'34"	58	148.3	4170	26.9	759	5.49	1075	60 $\pm$ 5 $N_f$ = 8.0 $W$ = 25%	252 $\pm$ 13 $N_f$ = 50.0 $W$ = 40%	–	$\chi^2$ = 62 $\nu$ = 55	–
WW8	Ma	48°19'13", 16°12'44"	47	269.7	5432	47.7	961	6.58	1304	144 $\pm$ 14 $N_f$ = 11.1 $W$ = 25%	262 $\pm$ 15 $N_f$ = 35.9 $W$ = 29%	–	$\chi^2$ = 57 $\nu$ = 44	–
WW10	Ma	48°10'32", 16°03'47"	60	301.0	7107	54.2	1279	6.6	1304	93 $\pm$ 8 $N_f$ = 6.9 $W$ = 21%	218 $\pm$ 18 $N_f$ = 32.2 $W$ = 27%	398 $\pm$ 53 $N_f$ = 20.9 $W$ = 34%	$\chi^2$ = 61 $\nu$ = 55	$P(F_{1,\nu}) = 0\%$ $F = 10.75$
<b>Kahlenberg nappe</b>														
WW6	Ma	48°15'32", 16°18'39"	55	263.7	7194	62.5	1705	6.53	1304	72 $\pm$ 6 $N_f$ = 5.7 $W$ = 19%	143 $\pm$ 9 $N_f$ = 23.2 $W$ = 23%	262 $\pm$ 14 $N_f$ = 26.1 $W$ = 26%	$\chi^2$ = 56 $\nu$ = 50	$P(F_{1,\nu}) = 0\%$ $F = 11.32$
WW4	Ca	48°16'25", 16°17'58"	60	92.8	5155	32.9	1832	5.46	1075	82 $\pm$ 4 $N_f$ = 44.4 $W$ = 23%	171 $\pm$ 16 $N_f$ = 15.6 $W$ = 30%	–	$\chi^2$ = 65 $\nu$ = 57	$P(F_{1,\nu}) = 0\%$ $F = 113.03$
WW7	a	48°16'38", 16°21'10"	25	202.0	1864	42.6	393	5.48	1075	76 $\pm$ 8 $N_f$ = 4.2 $W$ = 22%	220 $\pm$ 17 $N_f$ = 20.8 $W$ = 38%	–	$\chi^2$ = 27 $\nu$ = 22	–
	b		11	334.2	1061	52.6	167	6.48	1304	207 $\pm$ 22 $N_f$ = 7.7 $W$ = 29%	487 $\pm$ 113 $N_f$ = 3.3 $W$ = 45%	–	$\chi^2$ = 9.5 $\nu$ = 8	–
WW18	Ce–Tu	48°12'54", 16°12'22"	49	304.9	5293	61.2	1063	6.67	1325	119 $\pm$ 10 $N_f$ = 13.4 $W$ = 23%	267 $\pm$ 16 $N_f$ = 35.6 $W$ = 30%	–	$\chi^2$ = 54 $\nu$ = 46	–
<b>Laab nappe</b>														
WW15	Eo	48°03'54", 15°50'52"	60	294.2	7093	47.5	1144	6.67	1325	230 $\pm$ 12 $N_f$ = 50.7 $W$ = 28%	460 $\pm$ 97 $N_f$ = 9.3 $W$ = 39%	–	$\chi^2$ = 63 $\nu$ = 57	$P(F_{1,\nu}) = 0\%$ $F = 40.4$
WW11	Pa	48°01'45", 15°58'44"	60	338.6	8297	57.0	1397	6.67	1325	222 $\pm$ 16 $N_f$ = 40.8 $W$ = 25%	305 $\pm$ 38 $N_f$ = 19.2 $W$ = 29%	–	$\chi^2$ = 57 $\nu$ = 57	$P(F_{1,\nu}) = 0\%$ $F = 22.6$
WW13	Sa–Ca	48°03'11", 15°56'41"	60	310.6	6902	56.7	1261	6.64	1304	148 $\pm$ 12 $N_f$ = 15.0 $W$ = 24%	265 $\pm$ 14 $N_f$ = 45.0 $W$ = 30%	–	$\chi^2$ = 65 $\nu$ = 57	$P(F_{1,\nu}) = 0\%$ $F = 73.2$

Table 1 Continued

Sample No.	Sediment age [Myr]	Locality N, E	No. of Crystals	Spontaneous tracks		Induced tracks		Dosimeter glass		Age populations			Fit statistics
				$\rho_s$ [ $10^5 \text{ cm}^{-2}$ ]	$N_s$	$\rho_i$ [ $10^5 \text{ cm}^{-2}$ ]	$N_i$	$\rho_d$ [ $10^5 \text{ cm}^{-2}$ ]	$N_d$	Age $\pm 1\sigma$ [Myr]	$N_f$	$W$ [%]	
YB1	Sa–Ca	47°58'30", 14°55'50"	23	351.6	3523	73.8	739	6.67	1325	127 ± 9	282 ± 20	—	$\chi^2 = 23$ $\nu = 20$
										$N_f = 9.6$	$N_f = 13.4$	—	
YB3	Tu	47°57'52", 14°53'06"	46	347.6	6724	63.5	1229	6.66	1304	138 ± 11	251 ± 11	—	$\chi^2 = 44$ $\nu = 43$
										$N_f = 9.7$	$N_f = 36.3$	—	
										$W = 2.2\%$	$W = 25\%$	—	

$\rho$  = track density,  $N$  = number of counted tracks,  $N_f$  = number of grains in the age population,  $W$  = relative standard deviation,  $\chi^2$  = goodness-of-fit parameter,  $\nu$  = degrees of freedom,  $F$  = level of significance for peak 2 or 3, Ce = Cenomanian, Tu = Turonian, Co = Coniacian, Sa = Santonian, Ca = Campanian, Ma = Maastrichtian, Pa = Palaeocene, Eo = Eocene.

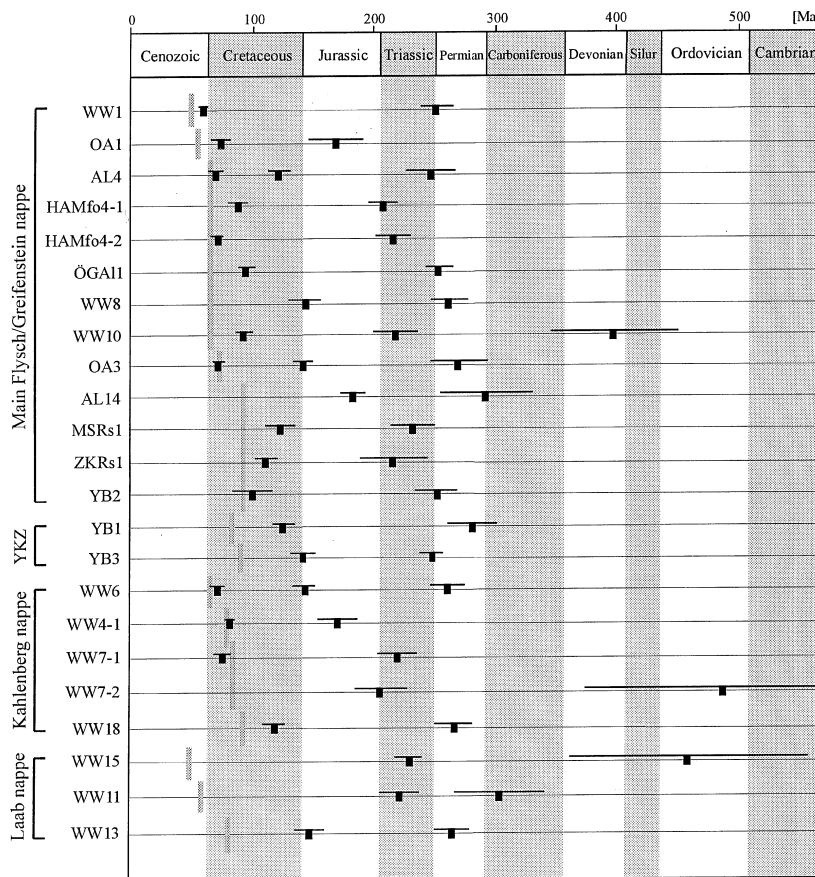


Fig. 3 Modelled zircon FT age clusters (age  $\pm 1\sigma$ ) using the computer program Binomfit (Brandon, 1992). Grey bars indicate sedimentation ages. YZK, Ybbsitz klippen zone.

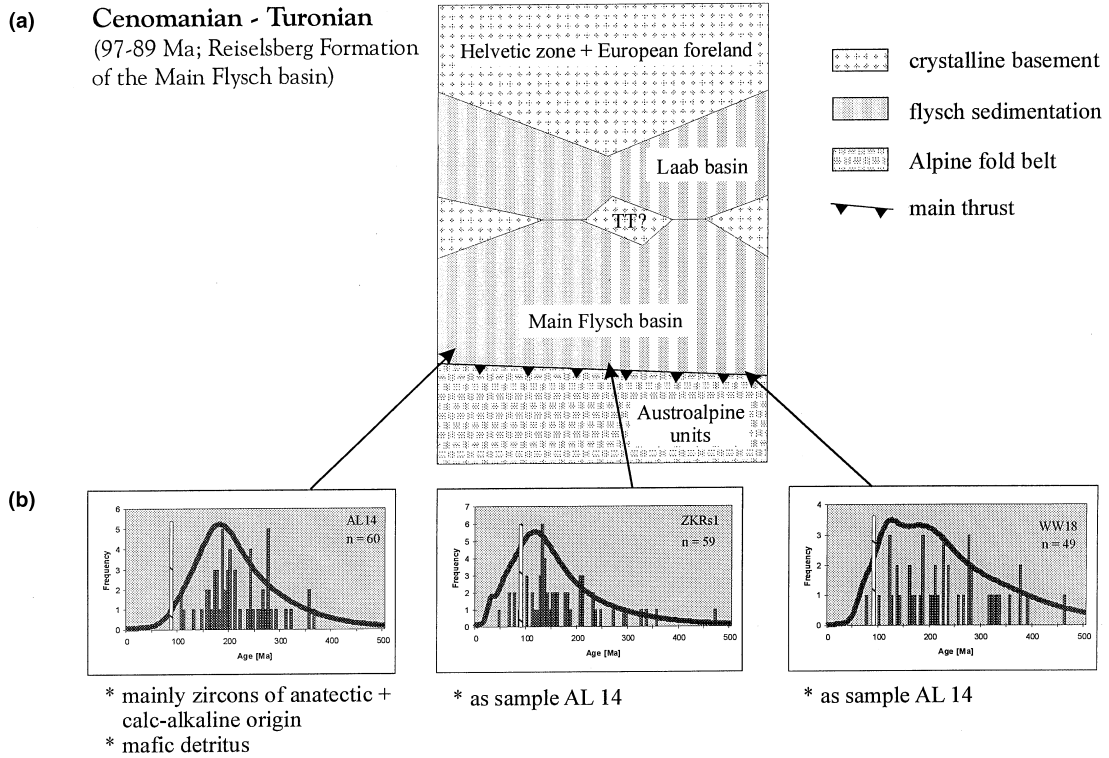
sediments nearly exclusively from a non-Alpine source or a source area in the Alps, which had not been affected by Eoalpine metamorphism.

*Maastrichtian–early Palaeocene (74–61 Ma)*

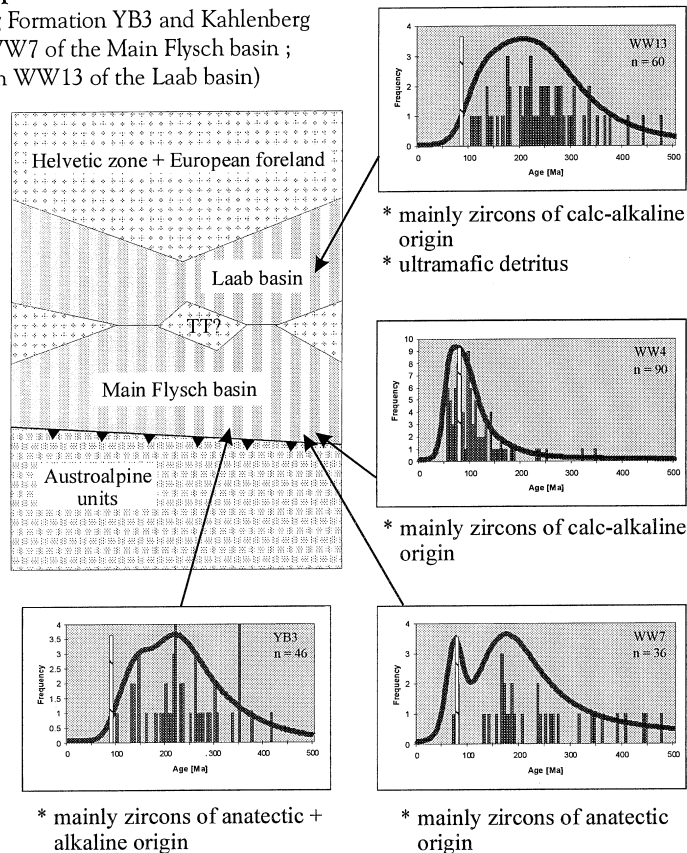
In Maastrichtian times, the source areas appear unchanged (Fig. 5a). The formations of the Main Flysch and Kahlenberg nappes show age distributions reflecting the Austroalpine Eoalpine event. Areas showing the age cluster around 70–90 Myr were eroded mainly in Maastrichtian times. The Palaeocene part of the Altengbach Formation in the Wienerwald contains reworked Triassic coal (Sachsenhofer, pers. comm.), which is known from the Lunzer Sandstein in the Northern Calcareous Alps. This supports the conclusion of an Austroalpine source for the sandstones of the Main Flysch/Greifenstein nappe.

*Late Palaeocene–early Eocene (61–45 Ma)*

The zircons of the Greifenstein Formation suggest a slightly different history (Fig. 5b). The FT age spectrum of sample WW1 is characterized by clusters around 60 and 250 Myr. The 60 Myr cluster contains colourless, euhedral to subhedral zircons. The short lag time between FT and sedimentation age suggests either a volcanic source or a fastly exhuming magmatic body. Similar zircon ages of  $\approx 58$  Myr in early late Palaeocene bentonites of the Swiss Schlieren flysch (Winkler *et al.*, 1990), and the euhedral shape of the crystals make a volcanic source most probable. Bentonite layers are also described in the Rhodanubian flysch zone near Salzburg and in the Northern Calcareous Alps (Egger, 1995; Egger *et al.*, 1996). Winkler *et al.* (1985) suggested an origin of these ashes in a volcanic



**Santonian - Campanian**  
(87-74 Ma; Hubberg Formation YB3 and Kahlenberg Formation WW4, WW7 of the Main Flysch basin ; Kaumberg Formation WW13 of the Laab basin)



centre south of the Alpine orogen. It is assumed herein that the zircons derived from tuffitic material in the source area (e.g. the Northern Calcareous Alps) or in the flysch basin itself.

The Palaeocene and Eocene rocks of the Laab nappe show age spectra which lack the young peak (samples WW15, WW11; Fig. 5b). They display age clusters > 220 Myr.

The southern margin of the BM was affected by enhanced heat flow during Permo-Triassic break-up of Pangaea and crustal thinning in this area. Thus, the increase of zircon FT ages with decreasing sedimentation age can, for instance, be explained by northward enlargement of the catchment area into regions that were unaffected by Permian–Triassic heat flow. The BM experienced latest Cretaceous–Palaeogene uplift (Hejl *et al.*, 1997).

## Discussion

Using the zircon FT data as provenance indicators, two depositional areas can be differentiated, which are defined herein as Main Flysch and Laab realm. The Main Flysch realm is characterized by detritus from the Eoalpine orogen, which underwent Cretaceous cooling after metamorphism. The Laab realm, in contrast, did not receive any sediments reflecting the Eoalpine event; thus, we argue that their source is in the BM. These conclusions, based on geochronological data, contrast with current ideas (e.g. Faupl, 1996), which assume three separate basins for the three different nappes in the Wienerwald area. The arguments for a subdivision into three basins are based mainly on palaeocurrent and heavy mineral data.

The Rhenodanubian flysch zone was involved in nappe stacking and late-collisional tectonic extrusion of the Eastern Alps (e.g. Ratschbacher *et al.*, 1991). Therefore, differential

block rotations – as in other parts of the Eastern Alps (e.g. Márton *et al.*, 2000) – may have obscured information about the original palaeocurrent pattern. The model of a long, narrow trough with dominantly longitudinal sedimentary transport (Hesse, 1972) is not in conflict with the present data. However, the assumption of an eastern and a western source area (Hesse, 1972) appears to be too schematic, as it is well known from flysch basins that radial supply is turned into longitudinal transport in the trough (Ricci Lucchi, 1985). Sedimentological investigations of Mattern (1998) indicate that a number of turbidite fan systems of the Reiselsberg Formation were supplied from a southern source.

Lithological similarities of the Reiselsberg Formation in the Main Flysch nappe and the Kahlenberg nappe (Egger, 1990) support the assumption of a continuous basin. Furthermore, Faupl (1996) found good correspondence of the Kahlenberg Formation (Kahlenberg nappe) and the Zementmergel Formation (Main Flysch/Greifenstein nappe). It is therefore assumed herein that the Kahlenberg nappe is derived from the southern part of the Main Flysch trough. Similar correlations with the YKZ suggest continuity with the Kahlenberg nappe (Decker, 1990; Egger, 1990; Schnabel, 1992).

The Laab realm is restricted to the Wienerwald area. According to the generally old zircon FT age populations ( $\geq$  Jurassic), a stable source area, which was not affected by Eoalpine metamorphism, supplied the Laab basin over a period of 30 Myr. A source area in the active Alpine orogen can be excluded, because the parts with very low-grade Eoalpine overprint (Silvretta, Fig. 1) were too far away. The Laab basin is therefore placed north of the Main Flysch basin. Sediment supply came from a northern source area. Undeformed coalified plant detritus, which is similar to Permian–Carboniferous coals in the BM (Boskowitz trough, Permian of Zöbing; Sachsenhofer, pers. comm.), supports these conclusions.

## Conclusions

Two palaeogeographic settings, which fit the geochronological data, are conceivable for the eastern RDFZ.

**1** Because the Laab realm did not receive detritus reflecting the Eoalpine orogeny, the two realms were separated by a basement high (Fig. 6a), called the Rhenodanubian high by Oberhauser (1995), who first described such a basin configuration. The question arises: is this basement high represented by the Tauern terrane in Middle Penninic position? (Frisch, 1979).

**2** A basement high is not necessary to explain the existing geochronological dataset. A single basin is conceivable, if the sediments of the Laab nappe were deposited at the European margin in less deep water than those of the Main Flysch nappe (Fig. 6b). A sediment transfer from the Laab to the Main Flysch sedimentation area was therefore possible, but not vice versa.

The exact position of the Rhenodanubian flysch zone within the Penninic realm is still under discussion (e.g. Frisch, 1979; Egger, 1992; Oberhauser, 1995). Integrating former ideas and the zircon data presented herein, four palaeogeographic configurations are possible:

**1** The Laab realm belongs to the North Penninic basin and is separated from the Main Flysch realm, which is part of the South Penninic ocean (cf. Oberhauser, 1995), by the Tauern terrane (e.g. Frisch, 1979) (Fig. 6d). The North and South Penninic basins have evolved in Jurassic to Cretaceous times (Frisch, 1979).

**2** The Rhenodanubian flysch was deposited entirely in the North Penninic realm (Frisch, 1979), and sedimentary supply of zircons from the Austroalpine zone into the Main Flysch realm occurred through channel ways east and west of the Tauern terrane (Fig. 6e).

**3** The South Penninic realm was closed earlier and the North Penninic basin directly received sediments from the Austroalpine units from the Cenomanian on (Fig. 6c).

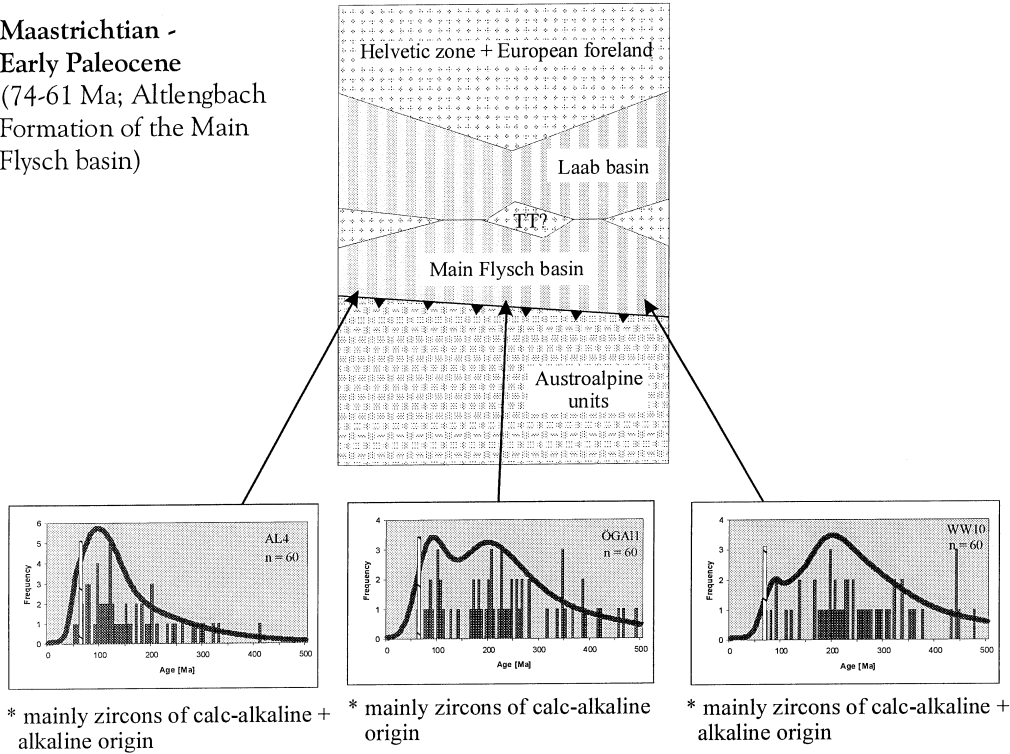
**4** The subdivision in a North and South Penninic basin did not exist in the eastern Alpine area (e.g. Hawkesworth *et al.*, 1975; Polino *et al.*, 1990), and the Rhenodanubian flysch was deposited in a single basin (Fig. 6b).

According to the data presented herein, possibility (4) is preferred, because this basin configuration enables accretion of the Rhenodanubian flysch

**Fig. 4** Arrangement of the source terrains of the Rhenodanubian flysch zone and the Ybbsitz klippen zone in Cenomanian to Campanian times. Plots show the single zircon fission-track grain ages in a histogram and the probability density curve (Hurford *et al.*, 1984) for the different formations. The white bar indicates the sedimentation age of each sample. TT, Tauern terrane.



(a) Maastrichtian - Early Paleocene (74-61 Ma; Altengbach Formation of the Main Flysch basin)



(b) Late Paleocene - Early Eocene (61-45 Ma; Greifenstein Formation OA1, WW1 of the Main Flysch basin, Laab Formation WW1, WW 15 of the Laab basin)

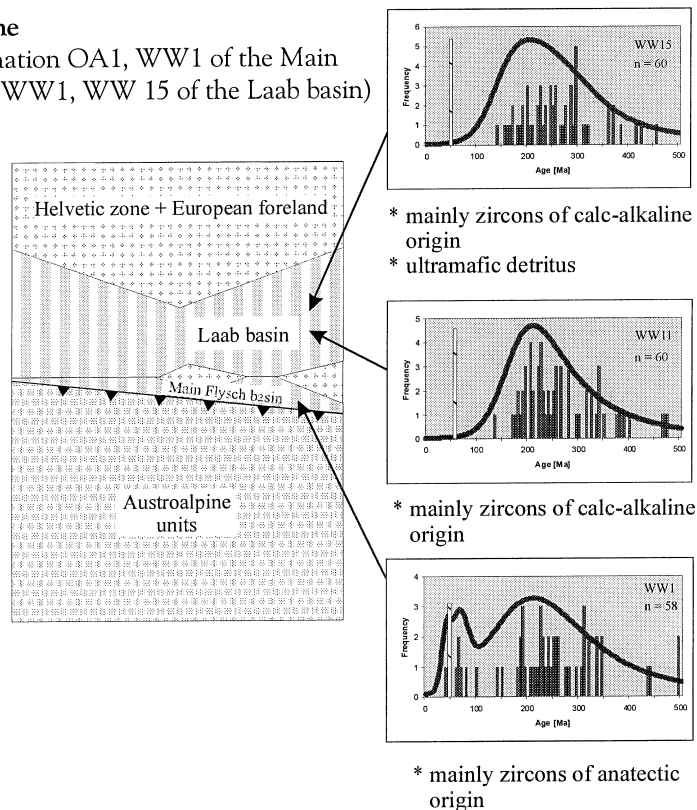
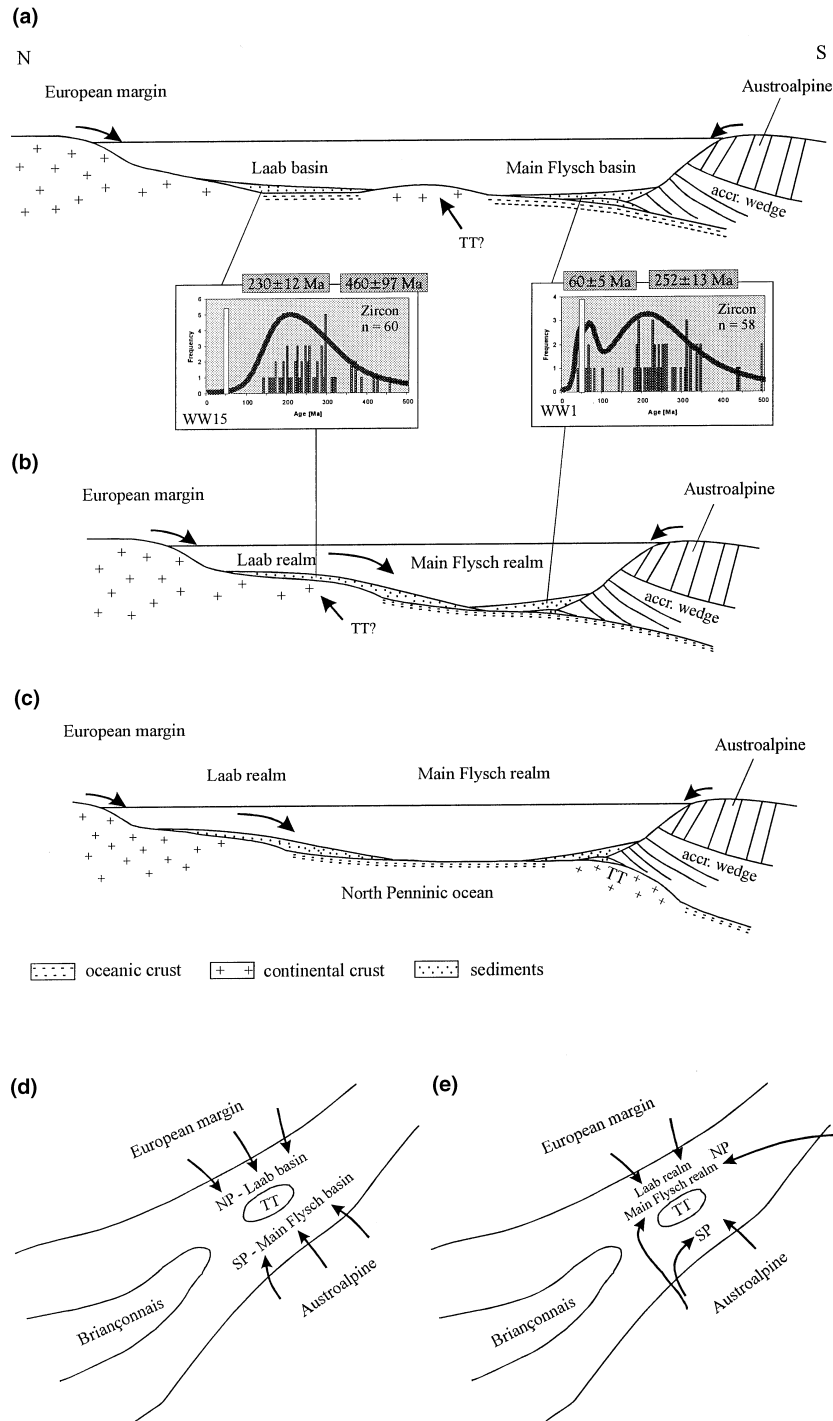


Fig. 5 Arrangement of the source terrains of the Rhenodanubian flysch zone in Maastrichtian to early Eocene times. Further explanation as in Fig. 4.



**Fig. 6** Palaeogeographical reconstructions of the Rhenodanubian flysch basin in Eocene times: (a) the two basins are separated by a submarine swell; (b) the Laab and Main Flysch depositional areas form a coherent depositional area basin, but due to the higher position of the Laab realm it does not receive detritus from the Alps.

Position of the Rhenodanubian flysch in the Penninic realm in Cenomanian to Eocene times: (b) The subdivision into a North and South Penninic ocean in the eastern Alpine area did not exist. The RDF was deposited in a single basin. (c) The RDF is deposited in the North Penninic realm and received sediments from the Austroalpine units since Cenomanian times owing to earlier closure of the South Penninic ocean. (d) The Main Flysch basin is situated in the South Penninic realm (SP), and the Laab basin in the North Penninic realm (NP). (e) The Rhenodanubian flysch is deposited entirely in the North Penninic realm with input from the east and west. TT, Tauern terrane.

before Maastrichtian times (Trautwein et al., 2000a) and grain supply from the BM into the Main Flysch basin.

### Acknowledgements

We are grateful to F. Moser, R. Sachsenhofer, M. Schwab and C. Spiegel for fruitful discussions, and T. Hurford and G. Dal Piaz for constructive reviews. Financial support from the German Science Foundation, the German Academic Exchange Service and the state Baden-Württemberg is gratefully acknowledged.

### References

- Bertotti, G., Seward, D., Wijbrans, J. et al., 1999. Crustal thermal regime prior to, during, and after rifting: a geochronological and modeling study of the Mesozoic South Alpine rifted margin. *Tectonics*, **18**, 185–200.
- Brandon, M.T., 1992. Decomposition of fission-track grain-age distributions. *Am. J. Sci.*, **292**, 535–564.
- Brügel, A., 1998. Provenance of alluvial conglomerates from the Eastalpine foreland: Oligo-/Miocene denudation history and drainage evolution of the Eastern Alps. *Tübinger Geowiss. Arb.*, **A40**, 1–168.
- Decker, K., 1990. Plate tectonics and pelagic facies: Late Jurassic to Early Cretaceous deep-sea sediments of the Ybbsitz ophiolite unit (Eastern Alps, Austria). *Sediment. Geol.*, **67**, 85–99.
- Dunkl, I., Frisch, W. and Kuhlemann, J., 1999. Fission track record of the thermal evolution of the Eastern Alps – review of the main zircon age clusters and the significance of the 160 Ma event. *Tübinger Geowiss. Arb.*, **A52**, 77–78.
- Egger, H., 1990. Zur paläogeographischen Stellung des Rhenodanubischen Flysches (Neokom-Eozän) der Ostalpen. *Jb. Geol. B.-A.*, **133**, 147–155.
- Egger, H., 1992. Zur Geodynamik und Paläogeographie des Rhenodanubischen Flysches (Neokom – Eozän) der Ostalpen. *Z. dt. Geol. Ges.*, **143**, 51–65.
- Egger, H., 1995. Zur Lithostratigraphie der Altengbach-Formation und der Anthering-Formation im Rhenodanubischen Flysch (Ostalpen, Penninikum). *N. Jb. Geol. Paläont.*, **196**, 69–91.
- Egger, H., Bichler, M., Homayoun, M. et al., 1996. Spätpaläozäne Bentonite aus der Gosau-Gruppe des Untersberg-Vorlandes (nördliche Kalkalpen, Salzburg). *Jb. Geol. B.-A.*, **139**, 13–20.
- von Eynatten, H., 1996. *Provenanzanalyse kretazischer Siliziklastika aus den Nördlichen Kalkalpen*. Unpubl. doctoral dissertation, University of Mainz.
- Faupl, P., 1996. Tiefwassersedimente und tektonischer Bau der Flyschzone des Wienerwaldes. In: *11th Sedimentologentreffen Wien, Exkursionsführer Sediment '96*. Geologische Bundesanstalt, Vienna.
- Frank, W., Kralik, M., Scharbert, S. et al., 1987. Geochronological data from the Eastern Alps. In: *Geodynamics of the Eastern Alps* (H.W. Flügel and P. Faupl, eds), pp. 379–406. Deuticke, Vienna.
- Frisch, W., 1979. Tectonic progradation and plate tectonic evolution of the Alps. *Tectonophysics*, **60**, 121–139.
- Galbraith, R.F. and Green, P.F., 1990. Estimating the component ages in a finite mixture. *Nucl. Tracks Rad. Meas.*, **17**, 207–214.
- Gleadow, A.J.W., Hurford, A.J. and Quaipe, R.D., 1976. Fission track dating of zircon: improved etching techniques. *Earth Planet. Sci. Lett.*, **33**, 273–276.
- Gleadow, A.J.W., 1981. Fission track dating methods: What are the real alternatives? *Nucl. Tracks*, **5**, 3–14.
- Gmach, H., 1999. *Thermische Reife der Flyschzone im Bereich des Wienerwaldes und der Flyschanteile nördlich der Donau und deren Einfluß auf die Kohlenwasserstoffgenese am Rand des Wiener Beckens*. Unpubl. diploma dissertation, University of Leoben.
- Hawkesworth, C.J., Waters, D.J. and Bickle, M.J., 1975. Plate tectonics in the Eastern Alps. *Earth Planet. Sci. Lett.*, **24**, 405–413.
- Hejl, E., Coyle, D., Lal, N. et al., 1997. Fission-track dating of the western border of the Bohemian massif: thermochronology and tectonic implications. *Geol. Rdsch.*, **86**, 210–219.
- Hesse, R., 1972. Lithostratigraphie, Petrographie und Entstehungsbedingungen des bayerischen Flysches: Unterkreide. *Geol. Bavarica*, **66**, 148–222.
- Hesse, R., 1973. Flysch-Gault und Falknistasna-Gault (Unterkreide): Kontinuierlicher Übergang von der distalen zur proximalen Flyschfazies auf einer penninischen Trogebene der Alpen. *Geol. Palaeont., Marburg*, **2**, 1–90.
- Hoinkes, G., Koller, F., Rantitsch, G. et al., 1999. Alpine metamorphism of the Eastern Alps. *Schweiz. Miner. Petrogr. Mitt.*, **79**, 155–181.
- Hurford, A.J., Fitch, F.J. and Clarke, A., 1984. Resolution of the age structure of the detrital zircon populations of two Lower Cretaceous sandstones from the Weald of England by fission track dating. *Geol. Mag.*, **121**, 269–277.
- Hurford, A.J., 1986. Cooling and uplift patterns in the Lepontine Alps South Central Switzerland and an age of vertical movement on the Insubric fault line. *Contr. Miner. Petrol.*, **92**, 413–427.
- Márton, E., Kuhlemann, J., Frisch, W. et al., 2000. Miocene rotations in the Eastern Alps; palaeomagnetic results from intramontane basin sediments. *Tectonophysics*, **323**, 163–182.
- Mattern, F., 1998. Lithostratigraphie und Fazies des Reiselberger Sandsteins: sandreiche, submarine Fächer (Cenomanium-Turonium, westlicher Rhenodanubischer Flysch, Ostalpen). *Berl. Geowiss. Abh.*, **A198**, 1–133.
- Neubauer, F., Hoinkes, G., Sassi, F.P. et al., 1999. Pre-Alpine metamorphism of the Eastern Alps. *Schweiz. Miner. Petrogr. Mitt.*, **79**, 41–62.
- Oberhauser, R., 1995. Zur Kenntnis der Tektonik und der Paläogeographie des Ostalpenraumes zur Kreide-, Paleozän- und Eozänzeit. *Jb. Geol. B.-A.*, **138**, 369–432.
- Petschick, R., 1989. Zur Wärmegeschichte im Kalkalpin Bayerns und Nordtirols (Inkohlung und Illit-Kristallinität). *Frankf. Geowiss. Arb. C*, **10**, 259 pp.
- Polino, R., Dal Piaz, G.V. and Gosso, G., 1990. Tectonic erosion at the Adria margin and accretionary processes for the Cretaceous orogeny of the Alps. *Mém. Soc. Géol. Fr.*, **156**, 345–367.
- Prey, S., 1973. Der südöstlichste Teil der Flyschzone bei Wien, ausgehend von der Bohrung Flötzersteig 1. *Verh. Geol. B.-A.*, **1972**, 67–94.
- Prey, S., 1983. Die Deckschollen der Kahlenberger Decke von Hochrotherd und Wolfsgraben im Wienerwald. *Verh. Geol. B.-A.*, **1982**, 243–250.
- Ratschbacher, L., Frisch, W. and Linzer, H.-G., 1991. Lateral extrusion in the Eastern alps, Part 2: Structural analysis. *Tectonics*, **10**, 257–271.
- Ricci Lucchi, F., 1985. Influence of transport processes and basin geometry on sand composition. In: *Provenance of Arenites* (G.G. Zuffa, ed.). *NATO ASI Series C*, **148**, 19–45.
- Ruttner, A. and Schnabel, W., 1988. *Geologische Karte der Republik Österreich, Blatt 71: Ybbsitz*, scale 1 : 50 000. Geol. B.-A, Vienna.
- Schnabel, W., 1992. New data on the Flysch Zone of the Eastern Alps in the Austrian sector and new aspects concerning the transition to the Flysch Zone of the Carpathians. *Cret. Res.*, **13**, 405–419.
- Schuster, R., Scharbert, S. and Abart, R., 1999. Permo-Triassic crustal extension during opening of the Neotethyan ocean in the Austroalpine-South Alpine realm. *Tübinger Geowiss. Arb.*, **A52**, 5–6.
- Thöni, M., 1999. A review of geochronological data from the Eastern Alps. *Schweiz. Miner. Petrogr. Mitt.*, **79**, 209–230.
- Trautwein, B., 2000. Detritus provenance and thermal history of the Rhenodanubian flysch zone: mosaicstones for the reconstruction of the geodynamic evolution.

- lution of the Eastern Alps. *Tübinger Geowiss. Arb.*, **A59**, 75 pp.
- Trautwein, B., Dunkl, I. and Frisch, W., 2001. Accretionary history of the Rhenodanubian flysch zone in the Eastern Alps – evidence from apatite fission-track geochronology. *Int. J. Earth Sci.*, **90**, 703–713.
- Vance, J., 1999. Zircon fission track evidence for a Jurassic (Tethyan) thermal event in the Western Alps. *Mem. Sci. Geol. Padova*, **51**, 473–476.
- Winkler, W., Galetti, G. and Maggetti, M., 1985. Bentonite im Gurnigel-, Schlieren- und Wägital-flysch: Mineralogie, Chemismus, Herkunft. *Eclog. Geol. Helv.*, **78**, 545–564.
- Winkler, W., Hurford, A.J., von Salis Perch-Nielsen, K. et al., 1990. Fission track and nannofossil ages from a Paleocene bentonite in the Schlieren Flysch (Central Alps, Switzerland). *Schweiz. Miner. Petrogr. Mitt.*, **70**, 389–396.
- Ziegler, P.A., 1988. Evolution of the Arctic-North Atlantic and the Western Tethys. *Mem. Am. Ass. Petrol. Geol.*, **43**, 1–198.

Received 22 February 2001; revised version accepted 4 September 2001